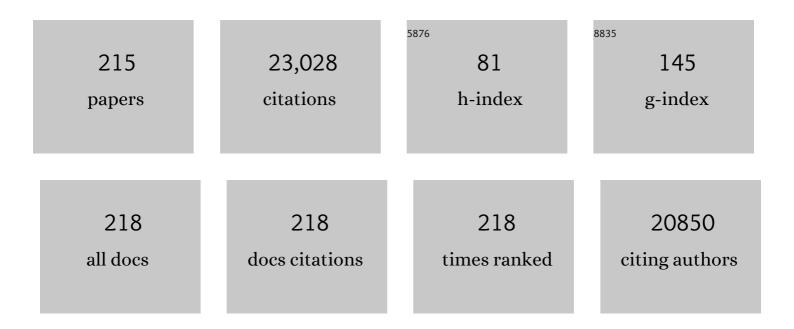
## Dai-Bin Kuang

List of Publications by Year in descending order

Source: https://exaly.com/author-pdf/848529/publications.pdf Version: 2024-02-01



#	Article	IF	CITATIONS
1	Ionic Liquids for the Convenient Synthesis of Functional Nanoparticles and Other Inorganic Nanostructures. Angewandte Chemie - International Edition, 2004, 43, 4988-4992.	7.2	1,127
2	A CsPbBr <sub>3</sub> Perovskite Quantum Dot/Graphene Oxide Composite for Photocatalytic CO <sub>2</sub> Reduction. Journal of the American Chemical Society, 2017, 139, 5660-5663.	6.6	946
3	Correlation between Photovoltaic Performance and Impedance Spectroscopy of Dye-Sensitized Solar Cells Based on Ionic Liquids. Journal of Physical Chemistry C, 2007, 111, 6550-6560.	1.5	870
4	Application of Highly Ordered TiO <sub>2</sub> Nanotube Arrays in Flexible Dye-Sensitized Solar Cells. ACS Nano, 2008, 2, 1113-1116.	7.3	630
5	High Molar Extinction Coefficient Heteroleptic Ruthenium Complexes for Thin Film Dye-Sensitized Solar Cells. Journal of the American Chemical Society, 2006, 128, 4146-4154.	6.6	538
6	Synthesis and Photocatalytic Application of Stable Leadâ€Free Cs <sub>2</sub> AgBiBr <sub>6</sub> Perovskite Nanocrystals. Small, 2018, 14, e1703762.	5.2	443
7	Stable Mesoscopic Dye-Sensitized Solar Cells Based on Tetracyanoborate Ionic Liquid Electrolyte. Journal of the American Chemical Society, 2006, 128, 7732-7733.	6.6	441
8	Novel porous molybdenum tungsten phosphide hybrid nanosheets on carbon cloth for efficient hydrogen evolution. Energy and Environmental Science, 2016, 9, 1468-1475.	15.6	437
9	Core@Shell CsPbBr <sub>3</sub> @Zeolitic Imidazolate Framework Nanocomposite for Efficient Photocatalytic CO <sub>2</sub> Reduction. ACS Energy Letters, 2018, 3, 2656-2662.	8.8	425
10	Reduced Graphene Oxide-Hierarchical ZnO Hollow Sphere Composites with Enhanced Photocurrent and Photocatalytic Activity. Journal of Physical Chemistry C, 2012, 116, 8111-8117.	1.5	413
11	Organic Dye‧ensitized Ionic Liquid Based Solar Cells: Remarkable Enhancement in Performance through Molecular Design of Indoline Sensitizers. Angewandte Chemie - International Edition, 2008, 47, 1923-1927.	7.2	389
12	Surfactant-Assisted Growth of Novel PbS Dendritic Nanostructures via Facile Hydrothermal Process. Advanced Materials, 2003, 15, 1747-1750.	11.1	361
13	Oriented hierarchical single crystalline anatase TiO <sub>2</sub> nanowire arrays on Ti-foil substrate for efficient flexible dye-sensitized solar cells. Energy and Environmental Science, 2012, 5, 5750-5757.	15.6	353
14	High-Efficiency and Stable Mesoscopic Dye-Sensitized Solar Cells Based on a High Molar Extinction Coefficient Ruthenium Sensitizer and Nonvolatile Electrolyte. Advanced Materials, 2007, 19, 1133-1137.	11.1	332
15	A Highly Redâ€Emissive Leadâ€Free Indiumâ€Based Perovskite Single Crystal for Sensitive Water Detection. Angewandte Chemie - International Edition, 2019, 58, 5277-5281.	7.2	310
16	In Situ Construction of a Cs <sub>2</sub> SnI <sub>6</sub> Perovskite Nanocrystal/SnS <sub>2</sub> Nanosheet Heterojunction with Boosted Interfacial Charge Transfer. Journal of the American Chemical Society, 2019, 141, 13434-13441.	6.6	303
17	Hierarchical Porous Silica Materials with a Trimodal Pore System Using Surfactant Templates. Journal of the American Chemical Society, 2004, 126, 10534-10535.	6.6	299
18	Hydrothermal Fabrication of Hierarchically Anatase TiO2 Nanowire arrays on FTO Glass for Dye-sensitized Solar Cells. Scientific Reports, 2013, 3, 1352.	1.6	291

#	Article	IF	CITATIONS
19	Tri-functional hierarchical TiO2 spheres consisting of anatase nanorods and nanoparticles for high efficiency dye-sensitized solar cells. Energy and Environmental Science, 2011, 4, 4079.	15.6	287
20	All-Solid-State Z-Scheme α-Fe2O3/Amine-RGO/CsPbBr3 Hybrids for Visible-Light-Driven Photocatalytic CO2 Reduction. CheM, 2020, 6, 766-780.	5.8	280
21	Bifacial dye-sensitized solar cells based on an ionic liquid electrolyte. Nature Photonics, 2008, 2, 693-698.	15.6	279
22	In Situ Growth of 120 cm <sup>2</sup> CH <sub>3</sub> NH <sub>3</sub> PbBr <sub>3</sub> Perovskite Crystal Film on FTO Glass for Narrowbandâ€Photodetectors. Advanced Materials, 2017, 29, 1602639.	11.1	252
23	Dynamic Study of Highly Efficient CdS/CdSe Quantum Dot-Sensitized Solar Cells Fabricated by Electrodeposition. ACS Nano, 2011, 5, 9494-9500.	7.3	249
24	Intrinsic Selfâ€Trapped Emission in 0D Leadâ€Free (C <sub>4</sub> H <sub>14</sub> N <sub>2</sub> ) <sub>2</sub> In <sub>2</sub> Br <sub>10</sub> Single Crystal. Angewandte Chemie - International Edition, 2019, 58, 15435-15440.	7.2	244
25	Z‣cheme 2D/2D Heterojunction of CsPbBr <sub>3</sub> /Bi <sub>2</sub> WO <sub>6</sub> for Improved Photocatalytic CO <sub>2</sub> Reduction. Advanced Functional Materials, 2020, 30, 2004293.	7.8	234
26	Multistack Integration of Three-Dimensional Hyperbranched Anatase Titania Architectures for High-Efficiency Dye-Sensitized Solar Cells. Journal of the American Chemical Society, 2014, 136, 6437-6445.	6.6	224
27	Ordered Crystalline TiO <sub>2</sub> Nanotube Arrays on Transparent FTO Glass for Efficient Dye-Sensitized Solar Cells. Journal of Physical Chemistry C, 2010, 114, 15228-15233.	1.5	201
28	Dimension engineering on cesium lead iodide for efficient and stable perovskite solar cells. Journal of Materials Chemistry A, 2017, 5, 2066-2072.	5.2	198
29	Co-sensitization of Organic Dyes for Efficient Ionic Liquid Electrolyte-Based Dye-Sensitized Solar Cells. Langmuir, 2007, 23, 10906-10909.	1.6	196
30	Improving the Extraction of Photogenerated Electrons with SnO <sub>2</sub> Nanocolloids for Efficient Planar Perovskite Solar Cells. Advanced Functional Materials, 2015, 25, 7200-7207.	7.8	194
31	Stable, Highâ€Efficiency Ionic‣iquidâ€Based Mesoscopic Dyeâ€Sensitized Solar Cells. Small, 2007, 3, 2094-210	025.2	191
32	Intrinsic Selfâ€Trapped Emission in OD Leadâ€Free (C <sub>4</sub> H <sub>14</sub> N <sub>2</sub> ) <sub>2</sub> In <sub>2</sub> Br <sub>10</sub> Single Crystal. Angewandte Chemie, 2019, 131, 15581-15586.	1.6	190
33	Ultra-long anatase TiO2nanowire arrays with multi-layered configuration on FTO glass for high-efficiency dye-sensitized solar cells. Energy and Environmental Science, 2014, 7, 644-649.	15.6	176
34	Principles of Hierarchical Meso- and Macropore Architectures by Liquid Crystalline and Polymer Colloid Templating. Langmuir, 2006, 22, 2311-2322.	1.6	169
35	Self-supported NiMoP <sub>2</sub> nanowires on carbon cloth as an efficient and durable electrocatalyst for overall water splitting. Journal of Materials Chemistry A, 2017, 5, 7191-7199.	5.2	168
36	Achieving high-performance planar perovskite solar cell with Nb-doped TiO <sub>2</sub> compact layer by enhanced electron injection and efficient charge extraction. Journal of Materials Chemistry A, 2016, 4, 5647-5653.	5.2	163

#	Article	IF	CITATIONS
37	Atomically Thin Defectâ€Rich Fe–Mn–O Hybrid Nanosheets as High Efficient Electrocatalyst for Water Oxidation. Advanced Functional Materials, 2018, 28, 1802463.	7.8	163
38	Fabrication of Novel Hierarchical β-Ni(OH) <sub>2</sub> and NiO Microspheres via an Easy Hydrothermal Process. Journal of Physical Chemistry C, 2009, 113, 5508-5513.	1.5	162
39	Effect of TiO2 morphology on photovoltaic performance of dye-sensitized solar cells: nanoparticles, nanofibers, hierarchical spheres and ellipsoid spheres. Journal of Materials Chemistry, 2012, 22, 7910.	6.7	162
40	Ion Coordinating Sensitizer for High Efficiency Mesoscopic Dye-Sensitized Solar Cells:  Influence of Lithium Ions on the Photovoltaic Performance of Liquid and Solid-State Cells. Nano Letters, 2006, 6, 769-773.	4.5	161
41	Maximizing omnidirectional light harvesting in metal oxide hyperbranched array architectures. Nature Communications, 2014, 5, 3968.	5.8	156
42	Metal-free organic dyes derived from triphenylethylene for dye-sensitized solar cells: tuning of the performance by phenothiazine and carbazole. Journal of Materials Chemistry, 2012, 22, 8994.	6.7	150
43	Highly efficient CdTe/CdS quantum dot sensitized solar cells fabricated by a one-step linker assisted chemical bath deposition. Chemical Science, 2011, 2, 1396.	3.7	148
44	High Molar Extinction Coefficient Ion-Coordinating Ruthenium Sensitizer for Efficient and Stable Mesoscopic Dye-Sensitized Solar Cells. Advanced Functional Materials, 2007, 17, 154-160.	7.8	147
45	All-Inorganic Lead-Free Cs <sub>2</sub> PdX <sub>6</sub> (X = Br, I) Perovskite Nanocrystals with Single Unit Cell Thickness and High Stability. ACS Energy Letters, 2018, 3, 2613-2619.	8.8	143
46	Multifunctional Phosphorus ontaining Lewis Acid and Base Passivation Enabling Efficient and Moisture‧table Perovskite Solar Cells. Advanced Functional Materials, 2020, 30, 1910710.	7.8	143
47	Hierarchically micro/nanostructured photoanode materials for dye-sensitized solar cells. Journal of Materials Chemistry, 2012, 22, 15475.	6.7	141
48	Organic Dye Bearing Asymmetric Double Donor-Ï€-Acceptor Chains for Dye-Sensitized Solar Cells. Journal of Organic Chemistry, 2011, 76, 8015-8021.	1.7	140
49	A micron-scale laminar MAPbBr <sub>3</sub> single crystal for an efficient and stable perovskite solar cell. Chemical Communications, 2017, 53, 5163-5166.	2.2	135
50	Enhanced Solar-Driven Gaseous CO <sub>2</sub> Conversion by CsPbBr <sub>3</sub> Nanocrystal/Pd Nanosheet Schottky-Junction Photocatalyst. ACS Applied Energy Materials, 2018, 1, 5083-5089.	2.5	135
51	Indium-antimony-halide single crystals for high-efficiency white-light emission and anti-counterfeiting. Science Advances, 2021, 7, .	4.7	134
52	All-Inorganic Lead-Free Heterometallic Cs4MnBi2Cl12 Perovskite Single Crystal with Highly Efficient Orange Emission. Matter, 2020, 3, 892-903.	5.0	133
53	An efficient organogelator for ionic liquids to prepare stable quasi-solid-state dye-sensitized solar cells. Journal of Materials Chemistry, 2006, 16, 2978-2983.	6.7	130
54	Influence of Ionic Liquids Bearing Functional Groups in Dye-Sensitized Solar Cells. Inorganic Chemistry, 2006, 45, 1585-1590.	1.9	130

#	Article	IF	CITATIONS
55	Fabrication of boehmite AlOOH and $\hat{I}^3$ -Al2O3 nanotubes via a soft solution route. Journal of Materials Chemistry, 2003, 13, 660-662.	6.7	128
56	A formamidinium–methylammonium lead iodide perovskite single crystal exhibiting exceptional optoelectronic properties and long-term stability. Journal of Materials Chemistry A, 2017, 5, 19431-19438.	5.2	126
57	Amorphousâ€TiO <sub>2</sub> â€Encapsulated CsPbBr <sub>3</sub> Nanocrystal Composite Photocatalyst with Enhanced Charge Separation and CO <sub>2</sub> Fixation. Advanced Materials Interfaces, 2018, 5, 1801015.	1.9	125
58	Understanding of carrier dynamics, heterojunction merits and device physics: towards designing efficient carrier transport layer-free perovskite solar cells. Chemical Society Reviews, 2020, 49, 354-381.	18.7	125
59	Hierarchical CsPbBr <sub>3</sub> nanocrystal-decorated ZnO nanowire/macroporous graphene hybrids for enhancing charge separation and photocatalytic CO <sub>2</sub> reduction. Journal of Materials Chemistry A, 2019, 7, 13762-13769.	5.2	115
60	An Overview for Zeroâ€Dimensional Broadband Emissive Metalâ€Halide Single Crystals. Advanced Optical Materials, 2021, 9, 2100544.	3.6	114
61	Sonochemical Preparation of Hierarchical ZnO Hollow Spheres for Efficient Dye ensitized Solar Cells. Chemistry - A European Journal, 2010, 16, 8757-8761.	1.7	111
62	Hierarchical Oriented Anatase TiO2 Nanostructure arrays on Flexible Substrate for Efficient Dye-sensitized Solar Cells. Scientific Reports, 2013, 3, 1892.	1.6	111
63	A Supercooled Imidazolium Iodide Ionic Liquid as a Low-Viscosity Electrolyte for Dye-Sensitized Solar Cells. Inorganic Chemistry, 2006, 45, 10407-10409.	1.9	104
64	Dye-sensitized solar cells based on a double layered TiO2 photoanode consisting of hierarchical nanowire arrays and nanoparticles with greatly improved photovoltaic performance. Journal of Materials Chemistry, 2012, 22, 18057.	6.7	100
65	Toward High Performance Photoelectrochemical Water Oxidation: Combined Effects of Ultrafine Cobalt Iron Oxide Nanoparticle. Advanced Functional Materials, 2016, 26, 4414-4421.	7.8	97
66	Enhanced On–Off Ratio Photodetectors Based on Leadâ€Free Cs <sub>3</sub> Bi <sub>2</sub> I <sub>9</sub> Single Crystal Thin Films. Advanced Functional Materials, 2020, 30, 1909701.	7.8	96
67	Recent Advances in Halide Perovskite Singleâ€Crystal Thin Films: Fabrication Methods and Optoelectronic Applications. Solar Rrl, 2019, 3, 1800294.	3.1	94
68	Preparation of inorganic salts (CaCO3, BaCO3, CaSO4) nanowires in the Triton X-100/cyclohexane/water reverse micelles. Journal of Crystal Growth, 2002, 244, 379-383.	0.7	92
69	In Situ Photosynthesis of an MAPbI <sub>3</sub> /CoP Hybrid Heterojunction for Efficient Photocatalytic Hydrogen Evolution. Advanced Functional Materials, 2020, 30, 2001478.	7.8	92
70	Electrospun Hierarchical TiO <sub>2</sub> Nanorods with High Porosity for Efficient Dye-Sensitized Solar Cells. ACS Applied Materials & Interfaces, 2013, 5, 9205-9211.	4.0	91
71	A double layered TiO2 photoanode consisting of hierarchical flowers and nanoparticles for high-efficiency dye-sensitized solar cells. Nanoscale, 2013, 5, 4362.	2.8	91
72	CdS/CdSe co-sensitized TiO2 nanowire-coated hollow Spheres exceeding 6% photovoltaic performance. Nano Energy, 2015, 11, 621-630.	8.2	91

#	Article	IF	CITATIONS
73	"Brick and Mortar―Strategy for the Formation of Highly Crystalline Mesoporous Titania Films from Nanocrystalline Building Blocks. Chemistry of Materials, 2009, 21, 1260-1265.	3.2	90
74	High performance and reduced charge recombination of CdSe/CdS quantum dot-sensitized solar cells. Journal of Materials Chemistry, 2012, 22, 12058.	6.7	90
75	Dithienopyrrolobenzothiadiazole-based organic dyes for efficient dye-sensitized solar cells. Journal of Materials Chemistry A, 2014, 2, 15365-15376.	5.2	90
76	Constructing 3D Branched Nanowire Coated Macroporous Metal Oxide Electrodes with Homogeneous or Heterogeneous Compositions for Efficient Solar Cells. Angewandte Chemie - International Edition, 2014, 53, 4816-4821.	7.2	90
77	Hierarchical Tin Oxide Octahedra for Highly Efficient Dyeâ€Sensitized Solar Cells. Chemistry - A European Journal, 2010, 16, 8620-8625.	1.7	86
78	Highly efficient and stable organic sensitizers with duplex starburst triphenylamine and carbazole donors for liquid and quasi-solid-state dye-sensitized solar cells. Journal of Materials Chemistry A, 2014, 2, 8988-8994.	5.2	84
79	A multifunctional poly-N-vinylcarbazole interlayer in perovskite solar cells for high stability and efficiency: a test with new triazatruxene-based hole transporting materials. Journal of Materials Chemistry A, 2017, 5, 1913-1918.	5.2	83
80	Phenothiazine-based dyes with bilateral extension of π-conjugation for efficient dye-sensitized solar cells. Dyes and Pigments, 2013, 96, 722-731.	2.0	82
81	Three-Dimensional TiO <sub>2</sub> /ZnO Hybrid Array as a Heterostructured Anode for Efficient Quantum-Dot-Sensitized Solar Cells. ACS Applied Materials & Interfaces, 2015, 7, 5199-5205.	4.0	82
82	Conformal coating of ultrathin metal-organic framework on semiconductor electrode for boosted photoelectrochemical water oxidation. Applied Catalysis B: Environmental, 2018, 237, 9-17.	10.8	82
83	High-performance light-driven heterogeneous CO2 catalysis with near-unity selectivity on metal phosphides. Nature Communications, 2020, 11, 5149.	5.8	82
84	CdS/CdSe co-sensitized vertically aligned anatase TiO2 nanowire arrays for efficient solar cells. Nano Energy, 2014, 8, 1-8.	8.2	81
85	Controllable Electrochemical Synthesis of Hierarchical ZnO Nanostructures on FTO Glass. Journal of Physical Chemistry C, 2009, 113, 13574-13582.	1.5	79
86	Trilateral π-conjugation extensions of phenothiazine-based dyes enhance the photovoltaic performance of the dye-sensitized solar cells. Dyes and Pigments, 2016, 124, 63-71.	2.0	75
87	Effect of the linkage location in double branched organic dyes on the photovoltaic performance of DSSCs. Journal of Materials Chemistry A, 2015, 3, 1333-1344.	5.2	72
88	Enhanced efficacy of defect passivation and charge extraction for efficient perovskite photovoltaics with a small open circuit voltage loss. Journal of Materials Chemistry A, 2019, 7, 9025-9033.	5.2	71
89	Plasmonic CsPbBr3–Au nanocomposite for excitation wavelength dependent photocatalytic CO2 reduction. Journal of Energy Chemistry, 2021, 53, 309-315.	7.1	70
90	A Review of Diverse Halide Perovskite Morphologies for Efficient Optoelectronic Applications. Small Methods, 2020, 4, 1900662.	4.6	69

#	Article	IF	CITATIONS
91	High-performance dye-sensitized solar cells based on hierarchical yolk–shell anatase TiO <sub>2</sub> beads. Journal of Materials Chemistry, 2012, 22, 1627-1633.	6.7	67
92	Activation of Selfâ€Trapped Emission in Stable Bismuthâ€Halide Perovskite by Suppressing Strong Exciton–Phonon Coupling. Advanced Functional Materials, 2021, 31, 2102654.	7.8	67
93	All-solid-state electrolytes consisting of ionic liquid and carbon black for efficient dye-sensitized solar cells. Journal of Photochemistry and Photobiology A: Chemistry, 2010, 216, 8-14.	2.0	66
94	CsPbBr <sub>3</sub> Nanocrystal/MO <sub>2</sub> (M = Si, Ti, Sn) Composites: Insight into Charge-Carrier Dynamics and Photoelectrochemical Applications. ACS Applied Materials & Interfaces, 2018, 10, 42301-42309.	4.0	66
95	Extraordinarily Efficient Conduction in a Redoxâ€Active Ionic Liquid. ChemPhysChem, 2011, 12, 145-149.	1.0	65
96	Hydrothermal fabrication of hierarchically macroporous Zn2SnO4 for highly efficient dye-sensitized solar cells. Nanoscale, 2013, 5, 5940.	2.8	65
97	Achieving Highly Efficient Photoelectrochemical Water Oxidation with a TiCl <sub>4</sub> Treated 3D Antimonyâ€Doped SnO <sub>2</sub> Macropore/Branched αâ€Fe <sub>2</sub> O <sub>3</sub> Nanorod Heterojunction Photoanode. Advanced Science, 2015, 2, 1500049.	5.6	65
98	The top-down synthesis of single-layered Cs <sub>4</sub> CuSb <sub>2</sub> Cl <sub>12</sub> halide perovskite nanocrystals for photoelectrochemical application. Nanoscale, 2019, 11, 5180-5187.	2.8	65
99	Dextran based highly conductive hydrogel polysulfide electrolyte for efficient quasi-solid-state quantum dot-sensitized solar cells. Electrochimica Acta, 2013, 92, 117-123.	2.6	64
100	Large-Area Synthesis of a Ni <sub>2</sub> P Honeycomb Electrode for Highly Efficient Water Splitting. ACS Applied Materials & Interfaces, 2017, 9, 32812-32819.	4.0	62
101	Macroporous SnO <sub>2</sub> Synthesized via a Template-Assisted Reflux Process for Efficient Dye-Sensitized Solar Cells. ACS Applied Materials & Interfaces, 2013, 5, 5105-5111.	4.0	61
102	Self-assembly of 2D Borromean networks through hydrogen-bonding recognition. Chemical Communications, 2009, , 2387.	2.2	59
103	Effect of Hydrocarbon Chain Length of Disubstituted Triphenyl-amine-Based Organic Dyes on Dye-Sensitized Solar Cells. Journal of Physical Chemistry C, 2011, 115, 22002-22008.	1.5	59
104	Zeroâ€Dimensional Znâ€Based Halides with Ultraâ€Long Roomâ€Temperature Phosphorescence for Timeâ€Resolved Antiâ€Counterfeiting. Angewandte Chemie - International Edition, 2022, 61, .	7.2	59
105	Novel dithieno[3,2-b:2′,3′-d]pyrrole-based organic dyes with high molar extinction coefficient for dye-sensitized solar cells. Organic Electronics, 2013, 14, 2071-2081.	1.4	58
106	Surface passivated halide perovskite single-crystal for efficient photoelectrochemical synthesis of dimethoxydihydrofuran. Nature Communications, 2021, 12, 1202.	5.8	58
107	A Highly Redâ€Emissive Leadâ€Free Indiumâ€Based Perovskite Single Crystal for Sensitive Water Detection. Angewandte Chemie, 2019, 131, 5331-5335.	1.6	57
108	A new ion-coordinating ruthenium sensitizer for mesoscopic dye-sensitized solar cells. Inorganica Chimica Acta, 2008, 361, 699-706.	1.2	56

#	Article	IF	CITATIONS
109	Large-scale planar and spherical light-emitting diodes based on arrays of perovskite quantum wires. Nature Photonics, 2022, 16, 284-290.	15.6	56
110	Performance of dye-sensitized solar cells based on novel sensitizers bearing asymmetric double Dâ~Ï€â~'A chains with arylamines as donors. Dyes and Pigments, 2012, 94, 481-489.	2.0	54
111	Morphology-controlled cactus-like branched anatase TiO2 arrays with high light-harvesting efficiency for dye-sensitized solar cells. Journal of Power Sources, 2014, 260, 6-11.	4.0	54
112	Ordered macroporous CH <sub>3</sub> NH <sub>3</sub> PbI <sub>3</sub> perovskite semitransparent film for high-performance solar cells. Journal of Materials Chemistry A, 2016, 4, 15662-15669.	5.2	54
113	A novel TCO- and Pt-free counter electrode for high efficiency dye-sensitized solar cells. Journal of Materials Chemistry A, 2013, 1, 1724-1730.	5.2	53
114	Asymmetric 3D Hole-Transporting Materials Based on Triphenylethylene for Perovskite Solar Cells. Chemistry of Materials, 2019, 31, 5431-5441.	3.2	53
115	Self-assembled lead-free double perovskite-MXene heterostructure with efficient charge separation for photocatalytic CO2 reduction. Applied Catalysis B: Environmental, 2022, 312, 121358.	10.8	53
116	Recent advances in hierarchical three-dimensional titanium dioxide nanotree arrays for high-performance solar cells. Journal of Materials Chemistry A, 2017, 5, 12699-12717.	5.2	52
117	Synthesis of hierarchical SnO2 octahedra with tailorable size and application in dye-sensitized solar cells with enhanced power conversion efficiency. Journal of Materials Chemistry, 2012, 22, 21495.	6.7	51
118	In situ formation of zinc ferrite modified Al-doped ZnO nanowire arrays for solar water splitting. Journal of Materials Chemistry A, 2016, 4, 5124-5129.	5.2	51
119	Immobilizing Re(CO) <sub>3</sub> Br(dcbpy) Complex on CsPbBr <sub>3</sub> Nanocrystal for Boosted Charge Separation and Photocatalytic CO <sub>2</sub> Reduction. Solar Rrl, 2020, 4, 1900365.	3.1	51
120	CdS/CdSe Quantum Dot Shell Decorated Vertical ZnO Nanowire Arrays by Spinâ€Coatingâ€Based SILAR for Photoelectrochemical Cells and Quantumâ€Dotâ€Sensitized Solar Cells. ChemPhysChem, 2012, 13, 1435-1439.	1.0	50
121	Mazeâ€Like Halide Perovskite Films for Efficient Electron Transport Layerâ€Free Perovskite Solar Cells. Solar Rrl, 2019, 3, 1800268.	3.1	49
122	The Electronic Role of the TiO2Light-Scattering Layer in Dye-Sensitized Solar Cells. Zeitschrift Fur Physikalische Chemie, 2007, 221, 319-327.	1.4	48
123	Three-dimensional hyperbranched TiO <sub>2</sub> /ZnO heterostructured arrays for efficient quantum dot-sensitized solar cells. Journal of Materials Chemistry A, 2015, 3, 14826-14832.	5.2	48
124	Inorganic cesium lead halide CsPbX3 nanowires for long-term stable solar cells. Science China Materials, 2017, 60, 285-294.	3.5	48
125	Synthesis of phenothiazine-based di-anchoring dyes containing fluorene linker and their photovoltaic performance. Dyes and Pigments, 2015, 114, 47-54.	2.0	47
126	Spontaneous surface/interface ligand-anchored functionalization for extremely high fill factor over 86% in perovskite solar cells. Nano Energy, 2020, 75, 104929.	8.2	47

#	Article	IF	CITATIONS
127	Solvent selection and Pt decoration towards enhanced photocatalytic CO <sub>2</sub> reduction over CsPbBr <sub>3</sub> perovskite single crystals. Sustainable Energy and Fuels, 2020, 4, 2249-2255.	2.5	47
128	Hydrothermal Fabrication of Quasiâ€Oneâ€Dimensional Singleâ€Crystalline Anatase TiO <sub>2</sub> Nanostructures on FTO Glass and Their Applications in Dye‣ensitized Solar Cells. Chemistry - A European Journal, 2011, 17, 1352-1357.	1.7	46
129	Hierarchical TiO2 flowers built from TiO2 nanotubes for efficient Pt-free based flexible dye-sensitized solar cells. Physical Chemistry Chemical Physics, 2012, 14, 13175.	1.3	46
130	A family of vertically aligned nanowires with smooth, hierarchical and hyperbranched architectures for efficient energy conversion. Nano Energy, 2014, 9, 15-24.	8.2	46
131	Trilayered Photoanode of TiO <sub>2</sub> Nanoparticles on a 1D–3D Nanostructured TiO <sub>2</sub> -Grown Flexible Ti Substrate for High-Efficiency (9.1%) Dye-Sensitized Solar Cells with Unprecedentedly High Photocurrent Density. Journal of Physical Chemistry C, 2014, 118, 16426-16432.	1.5	46
132	A novel metal–organic gel based electrolyte for efficient quasi-solid-state dye-sensitized solar cells. Journal of Materials Chemistry A, 2014, 2, 15406.	5.2	45
133	F-Type Pseudo-Halide Anions for High-Efficiency and Stable Wide-Band-Gap Inverted Perovskite Solar Cells with Fill Factor Exceeding 84%. ACS Nano, 2022, 16, 10798-10810.	7.3	45
134	Template-free solvothermal fabrication of hierarchical TiO2 hollow microspheres for efficient dye-sensitized solar cells. Journal of Materials Chemistry A, 2013, 1, 13274.	5.2	44
135	Hiearchical ZnO rod-in-tube nano-architecture arrays produced via a two-step hydrothermal and ultrasonication process. Journal of Materials Chemistry, 2011, 21, 8709.	6.7	43
136	Hierarchical Macroporous Zn <sub>2</sub> SnO <sub>4</sub> –ZnO Nanorod Composite Photoelectrodes for Efficient CdS/CdSe Quantum Dot Co-Sensitized Solar Cells. ACS Applied Materials & Interfaces, 2013, 5, 11865-11871.	4.0	43
137	Hierarchical Zn2SnO4 nanosheets consisting of nanoparticles for efficient dye-sensitized solar cells. Nano Energy, 2013, 2, 1287-1293.	8.2	42
138	Recent advances in hierarchical macroporous composite structures for photoelectric conversion. Energy and Environmental Science, 2014, 7, 3887-3901.	15.6	42
139	Room Temperature Fabrication of SnO <sub>2</sub> Electrodes Enabling Barrierâ€Free Electron Extraction for Efficient Flexible Perovskite Photovoltaics. Advanced Functional Materials, 2022, 32, .	7.8	42
140	Branched titania nanostructures for efficient energy conversion and storage: A review on design strategies, structural merits and multifunctionalities. Nano Energy, 2019, 62, 791-809.	8.2	41
141	Effect of polyphenyl-substituted ethylene end-capped groups in metal-free organic dyes on performance of dye-sensitized solar cells. RSC Advances, 2012, 2, 7788.	1.7	40
142	Electrospun TiO 2 nanofiber based hierarchical photoanode for efficient dye-sensitized solar cells. Electrochimica Acta, 2016, 189, 259-264.	2.6	39
143	Te4+-doped Cs2InCl5·H2O single crystals for remote optical thermometry. Science China Materials, 2022, 65, 764-772.	3.5	38
144	Stable dye-sensitized solar cells based on organic chromophores and ionic liquid electrolyte. Solar Energy, 2011, 85, 1189-1194.	2.9	36

#	Article	IF	CITATIONS
145	Anti-recombination organic dyes containing dendritic triphenylamine moieties for high open-circuit voltage of DSSCs. Dyes and Pigments, 2013, 99, 74-81.	2.0	35
146	Large-grained perovskite films via FA x MA 1â^'x Pb(I x Br 1â^'x ) 3 single crystal precursor for efficient solar cells. Nano Energy, 2017, 34, 264-270.	8.2	35
147	Tetraphenylbutadiene-Based Symmetric 3D Hole-Transporting Materials for Perovskite Solar Cells: A Trial Trade-off between Charge Mobility and Film Morphology. ACS Applied Materials & Interfaces, 2020, 12, 21088-21099.	4.0	35
148	Bright Cyanâ€Emissive Copper(I)â€Halide Single Crystals for Multiâ€Functional Applications. Advanced Optical Materials, 2022, 10, .	3.6	35
149	Iron-assisted engineering of molybdenum phosphide nanowires on carbon cloth for efficient hydrogen evolution in a wide pH range. Journal of Materials Chemistry A, 2017, 5, 22790-22796.	5.2	34
150	Constructing CsPbBr <sub>x</sub> I <sub>3â<sup>~?</sup>x</sub> nanocrystal/carbon nanotube composites with improved charge transfer and light harvesting for enhanced photoelectrochemical activity. Journal of Materials Chemistry A, 2019, 7, 5409-5415.	5.2	34
151	The Rise of Textured Perovskite Morphology: Revolutionizing the Pathway toward Highâ€Performance Optoelectronic Devices. Advanced Energy Materials, 2020, 10, 1902256.	10.2	34
152	Impact of hydroxy and octyloxy substituents of phenothiazine based dyes on the photovoltaic performance. Dyes and Pigments, 2013, 99, 299-307.	2.0	33
153	Influence of spatial arrangements of ï€-spacer and acceptor of phenothiazine based dyes on the performance of dye-sensitized solar cells. Organic Electronics, 2013, 14, 2662-2672.	1.4	33
154	Water-Molecule-Induced Emission Transformation of Zero-Dimension Antimony-Based Metal Halide. Inorganic Chemistry, 2022, 61, 338-345.	1.9	33
155	Facile Fabrication of Hierarchical SnO <sub>2</sub> Microspheres Film on Transparent FTO Glass. Inorganic Chemistry, 2010, 49, 1679-1686.	1.9	32
156	Novel organic dyes incorporating a carbazole or dendritic 3,6-diiodocarbazole unit for efficient dye-sensitized solar cells. Dyes and Pigments, 2014, 100, 269-277.	2.0	32
157	Porous ZnO@ZnSe nanosheet array for photoelectrochemical reduction of CO2. Electrochimica Acta, 2018, 274, 298-305.	2.6	32
158	Bladeâ€coating Perovskite Films with Diverse Compositions for Efficient Photovoltaics. Energy and Environmental Materials, 2021, 4, 277-283.	7.3	31
159	Stable organic dyes based on the benzo[1,2-b:4,5-bâ€2]dithiophene donor for efficient dye-sensitized solar cells. Journal of Materials Chemistry A, 2015, 3, 8083-8090.	5.2	30
160	Nonplanar Organic Sensitizers Featuring a Tetraphenylethene Structure and Double Electron-Withdrawing Anchoring Groups. Journal of Organic Chemistry, 2015, 80, 9034-9040.	1.7	30
161	Hydrophobic Hole-Transporting Materials Incorporating Multiple Thiophene Cores with Long Alkyl Chains for Efficient Perovskite Solar Cells. Electrochimica Acta, 2016, 209, 529-540.	2.6	29
162	Fabrication of a double layered photoanode consisting of SnO2 nanofibers and nanoparticles for efficient dye-sensitized solar cells. RSC Advances, 2013, 3, 13804.	1.7	28

#	Article	IF	CITATIONS
163	Synthesis of FeS2 and Co-doped FeS2 films with the aid of supercritical carbon dioxide and their photoelectrochemical properties. RSC Advances, 2011, 1, 255.	1.7	27
164	Highly Catalytic Carbon Nanotube/Pt Nanohybridâ€Based Transparent Counter Electrode for Efficient Dyeâ€Sensitized Solar Cells. Chemistry - an Asian Journal, 2012, 7, 1795-1802.	1.7	27
165	Starburst triarylamine based dyes bearing a 3,4-ethylenedioxythiophene linker for efficient dye-sensitized solar cells. Physical Chemistry Chemical Physics, 2013, 15, 11909.	1.3	26
166	Plasmonic silver nanoparticles matched with vertically aligned nitrogen-doped titanium dioxide nanotube arrays for enhanced photoelectrochemical activity. Journal of Power Sources, 2015, 274, 464-470.	4.0	26
167	D-A-ï€-A organic sensitizers containing a benzothiazole moiety as an additional acceptor for use in solar cells. Science China Chemistry, 2013, 56, 505-513.	4.2	25
168	Impact of the position isomer of the linkage in the double D–A branch-based organic dyes on the photovoltaic performance. Dyes and Pigments, 2014, 104, 89-96.	2.0	25
169	Understanding the charge transport properties of redox active metal–organic conjugated wires. Chemical Science, 2018, 9, 3438-3450.	3.7	25
170	Highly efficient and stable cyclometalated ruthenium(II) complexes as sensitizers for dye-sensitized solar cells. Electrochimica Acta, 2015, 174, 494-501.	2.6	24
171	Dyeâ€Sensitized Solar Cells with Improved Performance using <i>Cone</i> â€Calix[4]Arene Based Dyes. ChemSusChem, 2015, 8, 280-287.	3.6	24
172	Novel Ga-doped, self-supported, independent aligned ZnO nanorods: one-pot hydrothermal synthesis and structurally enhanced photocatalytic performance. RSC Advances, 2011, 1, 1691.	1.7	23
173	Synthesis and photovoltaic performance of asymmetric di-anchoring organic dyes. Dyes and Pigments, 2015, 122, 13-21.	2.0	22
174	High Photoluminescence Quantum Yield (>95%) of MAPbBr <sub>3</sub> Nanocrystals via Reprecipitation from Methylamine-MAPbBr <sub>3</sub> Liquid. ACS Applied Electronic Materials, 2020, 2, 2707-2715.	2.0	22
175	Synchronous surface and bulk composition management for red-shifted light absorption and suppressed interfacial recombination in perovskite solar cells. Journal of Materials Chemistry A, 2020, 8, 9743-9752.	5.2	22
176	Novel carbazole based sensitizers for efficient dye-sensitized solar cells: Role of the hexyl chain. Dyes and Pigments, 2015, 114, 18-23.	2.0	21
177	Hierarchical ZnO nanorod-on-nanosheet arrays electrodes for efficient CdSe quantum dot-sensitized solar cells. Science China Materials, 2016, 59, 807-816.	3.5	21
178	Simple hole-transporting materials containing twin-carbazole moiety and unconjugated flexible linker for efficient and stable perovskite solar cells. Chemical Engineering Journal, 2021, 405, 126434.	6.6	21
179	A laminar MAPbBr3/MAPbBr3â^'xlx graded heterojunction single crystal for enhancing charge extraction and optoelectronic performance. Journal of Materials Chemistry C, 2019, 7, 5670-5676.	2.7	20
180	Aâ€Site Diamine Cation Anchoring Enables Efficient Charge Transfer and Suppressed Ion Migration in Biâ€Based Hybrid Perovskite Single Crystals. Angewandte Chemie - International Edition, 2022, 61, .	7.2	20

#	Article	IF	CITATIONS
181	3,4â€Phenylenedioxythiophene (PheDOT) Based Holeâ€Transporting Materials for Perovskite Solar Cells. Chemistry - an Asian Journal, 2016, 11, 1043-1049.	1.7	19
182	Construction of a ternary WO3/CsPbBr3/ZIF-67 heterostructure for enhanced photocatalytic carbon dioxide reduction. Science China Materials, 2022, 65, 1550-1559.	3.5	19
183	Strongly Quantum-Confined Perovskite Nanowire Arrays for Color-Tunable Blue-Light-Emitting Diodes. ACS Nano, 2022, 16, 8388-8398.	7.3	19
184	Continuous Formation of Supported Unusual Mesostructured Silica Films by Solâ^'Gel Dip Coating. Langmuir, 2002, 18, 9570-9573.	1.6	18
185	In situ gelation of Al(III)-4-tert-butylpyridine based metal-organic gel electrolyte for efficient quasi-solid-state dye-sensitized solar cells. Journal of Power Sources, 2017, 343, 148-155.	4.0	18
186	Constructing a Cs <sub>3</sub> Sb <sub>2</sub> Br <sub>9</sub> /g <sub>3</sub> N <sub>4</sub> Hybrid for Photocatalytic Aromatic C( <i>sp</i> <sup>3</sup> )H Bond Activation. Solar Rrl, 2021, 5, 2100559.	3.1	18
187	Fabrication of partially crystalline TiO2 nanotube arrays using 1, 2-propanediol electrolytes and application in dye-sensitized solar cells. Advanced Powder Technology, 2013, 24, 175-182.	2.0	17
188	3D Cathodes of Cupric Oxide Nanosheets Coated onto Macroporous Antimonyâ€Đoped Tin Oxide for Photoelectrochemical Water Splitting. ChemSusChem, 2016, 9, 3012-3018.	3.6	17
189	CdS/CdSe co-sensitized hierarchical TiO <sub>2</sub> nanofiber/ZnO nanosheet heterojunction photoanode for quantum dot-sensitized solar cells. RSC Advances, 2016, 6, 78202-78209.	1.7	16
190	Solution-Processed Anatase Titania Nanowires: From Hyperbranched Design to Optoelectronic Applications. Accounts of Chemical Research, 2019, 52, 633-644.	7.6	16
191	Ruthenium dyes with heteroleptic tridentate 2,6-bis(benzimidazol-2-yl)-pyridine for dye-sensitized solar cells: Enhancement in performance through structural modifications. Inorganica Chimica Acta, 2012, 392, 388-395.	1.2	15
192	Bifacial Contact Junction Engineering for Highâ€Performance Perovskite Solar Cells with Efficiency Exceeding 21%. Small, 2019, 15, 1900606.	5.2	15
193	Emissionâ€Colorâ€Tunable Pbâ^'Sn Alloyed Single Crystals with High Luminescent Efficiency and Stability. Advanced Optical Materials, 2022, 10, .	3.6	15
194	Coordination disk-type nano-Saturn complexes. Chemical Communications, 2020, 56, 3325-3328.	2.2	14
195	Zeroâ€Dimensional Znâ€Based Halides with Ultraâ€Long Roomâ€Temperature Phosphorescence for Timeâ€Resolved Antiâ€Counterfeiting. Angewandte Chemie, 2022, 134, .	1.6	14
196	Fabrication of ordered macroporous rutile titania at low temperature. New Journal of Chemistry, 2002, 26, 819-821.	1.4	13
197	A Mild Oneâ€Step Process from Graphene Oxide and Cd <sup>2+</sup> to a Graphene–CdSe Quantum Dot Nanocomposite with Enhanced Photoelectric Properties. ChemPhysChem, 2012, 13, 2654-2658.	1.0	13
198	Synthesis and photovoltaic performance of dihydrodibenzoazepine-based sensitizers with additional lateral anchor. Dyes and Pigments, 2013, 99, 1072-1081.	2.0	13

#	Article	IF	CITATIONS
199	Hierarchical tree-like heterostructure arrays for enhanced photoeletrochemical activity. Electrochimica Acta, 2014, 136, 217-222.	2.6	13
200	Cooperative effects of Dopant-Free Hole-Transporting materials and polycarbonate film for sustainable perovskite solar cells. Chemical Engineering Journal, 2022, 437, 135197.	6.6	13
201	Novel phenanthroline-based ruthenium complexes for dye-sensitized solar cells: enhancement in performance through fluoro-substitution. RSC Advances, 2013, 3, 19311.	1.7	12
202	A facile method to fabricate high-quality perovskite nanocrystals based on single crystal powder. Nano Research, 2019, 12, 2640-2645.	5.8	12
203	Rational Surface Engineering of Anatase Titania Core–Shell Nanowire Arrays: Full-Solution Processed Synthesis and Remarkable Photovoltaic Performance. ACS Applied Materials & Interfaces, 2014, 6, 19100-19108.	4.0	11
204	Ni x S y /NiSe 2 Hybrid Catalyst Grown In Situ on Conductive Glass Substrate as Efficient Counter Electrode for Dye-Sensitized Solar Cells. Electrochimica Acta, 2017, 250, 244-250.	2.6	11
205	In Situ Construction of Direct Zâ€6cheme Cs <sub><i>x</i></sub> WO <sub>3</sub> /CsPbBr <sub>3</sub> Heterojunctions via Cosharing Cs Atom. Solar Rrl, 2021, 5, 2100036.	3.1	11
206	Making nanometer thick silica glass scaffolds: an experimental approach to learn about size effects in glasses. Colloid and Polymer Science, 2004, 282, 892-900.	1.0	10
207	Layered-stacking of titania films for solar energy conversion: Toward tailored optical, electronic and photovoltaic performance. Journal of Energy Chemistry, 2018, 27, 690-702.	7.1	10
208	Engineering multinary heterointerfaces in two-dimensional cobalt molybdenum phosphide hybrid nanosheets for efficient electrocatalytic water splitting. Sustainable Energy and Fuels, 2021, 5, 3458-3466.	2.5	9
209	Multichromophoric di-anchoring sensitizers incorporating a ruthenium complex and an organic triphenyl amine dye for efficient dye-sensitized solar cells. Inorganic Chemistry Frontiers, 2015, 2, 1040-1044.	3.0	7
210	Hierarchical TiO <sub>2</sub> –B/anatase core/shell nanowire arrays for efficient dye-sensitized solar cells. RSC Advances, 2016, 6, 1288-1295.	1.7	6
211	Recent Advances in Halide Perovskite Singleâ€Crystal Thin Films: Fabrication Methods and Optoelectronic Applications (Solar RRL 4â^•2019). Solar Rrl, 2019, 3, 1970044.	3.1	5
212	0D/2D CsPbBr <sub>3</sub> Nanocrystal/BiOCl Nanoplate Heterostructure with Enhanced Photocatalytic Performance. Advanced Materials Interfaces, 2022, 9, .	1.9	3
213	Optoelectronic Devices: The Rise of Textured Perovskite Morphology: Revolutionizing the Pathway toward Highâ€Performance Optoelectronic Devices (Adv. Energy Mater. 7/2020). Advanced Energy Materials, 2020, 10, 2070029.	10.2	1
214	Aâ€Site Diamine Cation Anchoring Enables Efficient Charge Transfer and Suppressed Ion Migration in Biâ€based Hybrid Perovskite Single Crystals. Angewandte Chemie, 0, , .	1.6	1
215	Water Splitting: Achieving Highly Efficient Photoelectrochemical Water Oxidation with a TiCl <sub>4</sub> Treated 3D Antimonyâ€Doped SnO <sub>2</sub> Macropore/Branched αâ€Fe <sub>2</sub> O <sub>3</sub> Nanorod Heterojunction Photoanode (Adv. Sci. 7/2015). Advanced Science. 2015. 2	5.6	0